Observation of Single Helical Peptide Molecule Incorporated into Alkanethiol Self-Assembled Monolayer on Gold by Scanning Tunneling Microscopy

Kazuya Kitagawa, Tomoyuki Morita, and Shunsaku Kimura*

Department of Material Chemistry, Graduate School of Engineering, Kyoto University, Kyoto-Daigaku Katsura, Nishikyo-ku, Kyoto 615-8510, Japan

Received: April 16, 2004; In Final Form: June 25, 2004

The bicomponent self-assembled monolayers (SAMs) were formed by incorporation of helical peptides into the alkanethiol monolayer, which was prepared in advance on gold substrate, and were characterized by Fourier transform infrared reflection−absorption spectroscopy (FTIR RAS) and scanning tunneling microscopy (STM). FTIR RAS spectra showed that the helical peptides were incorporated into the defects in the alkanethiol SAM without disturbing the film structure. A single helical peptide molecule was observed clearly in the bicomponent SAMs by STM. Several helical peptides associated together in a parallel arrangement to form a helix-bundle structure. Observation of the long molecule of ∼4 nm length standing vertically on the surface indicated that electron transfer occurred over a long distance through the helical peptide under the STM conditions.

Introduction

An understanding of electron transfer through a single molecule or a group of molecules with a setup of two electrodes for current detection is of primary importance for realization of molecular electronics.[1−10] For the electronic circuit at a molecular level, various techniques such as break junction,[2] nanogap electrode,[3] mercury drop-metal junction,[4] nanopore junction,[5] metal wire crossing,[6] and scanning probe microscopy[7,8] have been utilized so far. These results have shown that the mechanism for electron transfer across molecules is dominantly governed by coherent electron tunneling. There is another mechanism, inelastic hopping electron transfer, however, which is crucially important in a long-range electron transfer because of the ohmic behavior instead of the exponential decay with distance of the coherent electron tunneling. For example, the long-range electron transfer in the biological molecules such as DNA and protein is explained by the hopping mechanism.[9]

Scanning probe microscopy (SPM) including scanning tunneling microscopy (STM) and conducting probe atomic force microscopy (CP-AFM) is a strong tool for both imaging an organic single molecule or a group of molecules on the surface and evaluating their current−voltage characteristics at the same time. Here we report for the first time the results of STM observation of a single helical peptide incorporated into an alkanethiol monolayer on the gold surface. α-Helical polypeptides have attracted much attention in view of electron transfer, because the α-helix should play some important roles for a long-range electron transfer between chromophores in the natural photosynthetic system.[10−12] Recently, the long-range electron transfer through the helical peptide over 4 nm has been demonstrated to occur according to the inelastic hopping mechanism via amide bonds.[12d] Further, it was shown that the electron transfer along the dipole moment was faster than that against the dipole moment, meaning the large dipole moment of the helical polypeptide influences the direction of electron transfer.[12] Helical peptides therefore have the high potential of a molecular diode which rectifies the current through the molecule in one direction. To gain information on electronic properties of helical peptides, the single molecule observation by SPM is of basic importance.

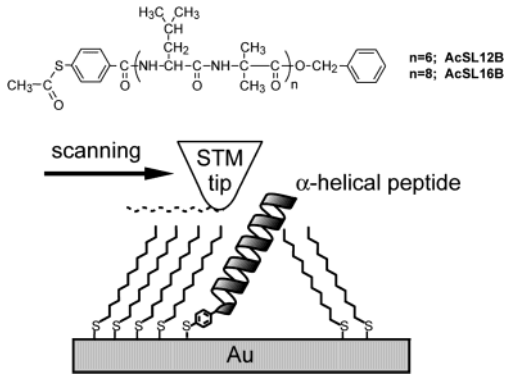

Figure 1. Molecular structure of the synthesized peptide and schematic illustration of STM observation of the bicomponent monolayer.

Two kinds of helical peptides of different chain lengths having a thioacetylphenyl group at the N terminal (AcSL12B, AcSL16B; Figure 1) were synthesized by the conventional liquid-phase method. These helical peptide SAMs or the bicomponent SAMs composed of helical peptides and alkanethiols were prepared on gold. The monolayers were characterized by Fourier transform infrared reflection−absorption spectroscopy (FTIR RAS) and ellipsometry and finally observed by ultrahigh vacuum scanning tunneling microscopy (UHV STM).[13]

Experimental Section

Synthesis of Helical Peptides. All chemicals were purchased from commercial suppliers and used without further purification. AcSL12B and AcSL16B were synthesized by a conventional liquid-phase method, and all intermediates and final products were identified by ^{1}H NMR, and their purity was checked by thin-layer chromatography (TLC). The final products were further confirmed by mass spectroscopy. ^{1}H NMR (400 MHz) spectra in $CDCl_3$ were measured by a Brucker AVANCE 400

* To whom correspondence should be addressed. Tel.: +81-75-383-2400. Fax: +81-75-383-2401. E-mail: shun@scl.kyoto-u.ac.jp.

10.1021/jp048333w CCC: $27.50
Published on Web 08/27/2004

spectrometer, and chemical shifts were given in δ value. Mass spectra were obtained by a JEOL JMS−HX110A spectrometer. TLC analyses were performed on Merck silica gel 60 F_{254} aluminum plates. Solvent systems for TLC were (A) chloroform/methanol/ammonia water (13/5/1 v/v/v), (B) chloroform/methanol (5/1 v/v), and (C) chloroform/methanol/acetic acid (95/5/3 v/v/v), respectively.

AcSL12B. After the Boc group of Boc-(L-Leu-Aib)$_6$-OBzl was removed by treatment with trifluoroacetic acid (TFA), the deprotected peptide was dissolved in chloroform and reacted with 4-(*S*-acetylthio)benzoic acid in the presence of *O*-(7-azabenzotriazol-1-yl)-1,1,3,3-tetramethyluronium hexafluorophosphate (HATU) and diisopropylethylamine (DIEA) at 0 °C for 30 min and thereafter at room temperature for 24 h. Then, the solution was evaporated and the crude product was purified twice by a Sephadex LH-20 column (methanol/chloroform 1/1 (v/v) as eluent). The fractionated solid was washed with *n*-hexane to afford the product as a white solid in 40% yield. ^{1}H NMR ($CDCl_3$, 400 MHz): δ(ppm) 0.72−0.98 (36H, m, Leu CδH_3), 1.23−1.75 (54H, brm, Aib CH_3, Leu CγH CβH_2), 2.41 (3H, s, CH_3C(=O)S), 3.95−4.14 (6H, m, Leu CαH), 4.95 (2H, s, benzyl CH_2), 7.28 (5H, m, benzene), 7.55, 8.12 (4H, d, aromatic) 7.18, 7.61−7.99, 9.15 (12H, brm, amide NH). FAB-MS: $[M+Na]^+$ 1497.8; Calcd for $C_{76}H_{122}O_{15}N_{12}SNa$, 1497.9. TLC: R_f(A) = 0.86, R_f(B) = 0.66, R_f(C) = 0.27.

AcSL16B. AcSL16B was synthesized similarly to AcSL12B. The crude product was purified twice by a Sephadex LH-20 column (methanol/chloroform 1/1 (v/v) as eluent). Washing the solid with *n*-hexane gave the white product in 20% yield. ^{1}H NMR ($CDCl_3$, 400 MHz): δ(ppm) 0.77−0.98 (48H, m, Leu CδH_3), 1.22−1.71 (72H, brm, Aib CH_3, Leu CγH CβH_2), 2.43 (3H, s, CH_3C(=O)S), 3.95−4.16 (8H, m, Leu CαH), 5.02 (2H, s, benzyl CH_2), 7.25 (5H, m, benzene), 7.60, 8.00 (4H, d, aromatic) 7.09, 7.52−8.08 (16H, brm, amide NH). FAB-MS: $[M+Na]^+$ 1895.1; Calcd for $C_{96}H_{158}O_{19}N_{16}SNa$, 1895.2. TLC: R_f(A) = 0.91, R_f(B) = 0.71.

Circular Dichroism (CD) Spectroscopy. CD spectra of the peptides in a trifluoroethanol solution were measured at room temperature on a JASCO J-600 CD spectropolarimeter using an optical cell of 0.1 cm path length.

SAMs Preparation. Gold substrates for RAS and ellipsometry were prepared by vapor deposition of chromium (50 nm) as adhesion layer and then gold (99.99%, 200 nm) on a slide glass. The slide glasses were cleaned ahead of deposition by using a piranha solution (H_2SO_4/H_2O_2 = 7/3), followed by rigorous rinsing with distilled water and methanol. In the case of gold substrates for STM studies, gold was deposited on the surface of freshly cleaved mica by thermal evaporation and then was annealed just before preparation of the SAMs.

The single-component SAMs of helical peptides were prepared by immersion of the gold substrate in an ethanol solution of the peptide (0.1 mM) for 24 h. The peptide was treated in advance with the addition of 5 μL of ammonia water (28 wt %) per 1 mg of the peptide to deblock the acetyl group. After incubation, the substrate was washed thoroughly with ethanol and dried in a stream of dry nitrogen gas. The bicomponent SAMs of alkanethiols and the helical peptides were prepared by immersion of an alkanethiolate SAM, which was prepared in advance from 1.0 mM alkanethiol in ethanol, into an ethanol or chloroform solution of the peptide (0.1 mM) for 24 h. After the incubation, the substrate was washed similarly to the preparation of the peptide SAMs.

FTIR RAS. FTIR RAS spectra were recorded on a Nicolet Magna 850 Fourier transform infrared spectrometer. For RAS measurements, a Harrick model RMA-1DG/VRA reflection attachment was used. Incident angle was set at 85°. The number of interferogram accumulations was 500. The molecular orientation of the peptide monolayer on gold was determined on the basis of the amide I/amide II absorbance ratio in the FTIR RAS spectrum according to eq 1 under an assumption of a uniform distribution of the helical peptides along the surface normal[14]

$$\frac{I_1}{I_2} = C\frac{2\left[\frac{1}{2}(3\cos^2\gamma - 1)\right]\left[\frac{1}{2}(3\cos^2\theta_1 - 1)\right] + 1}{2\left[\frac{1}{2}(3\cos^2\gamma - 1)\right]\left[\frac{1}{2}(3\cos^2\theta_2 - 1)\right] + 1} \quad (1)$$

where I_i, C, γ, and θ_i (i = 1 or 2 corresponds to amide I or amide II) represent the observed absorbance, the scaling constant (C = 1.5 for the peptides), the tilt angle of the helix axis from the surface normal, and the angle between the transition moment of amide vibration mode and the helix axis, respectively. The values of θ_1 and θ_2 were taken to be 39 and 75°, respectively.[15]

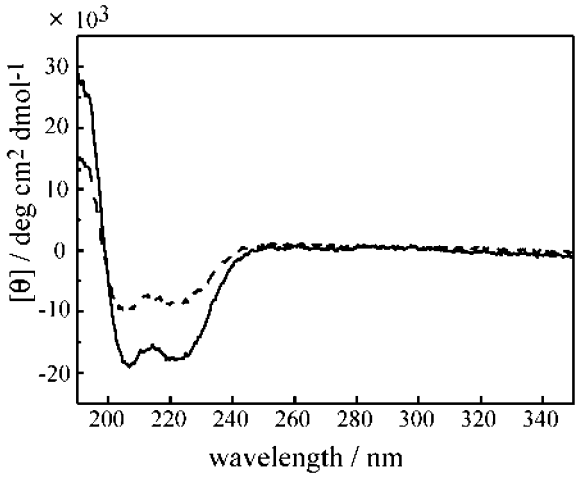

Figure 2. CD spectra of AcSL12B (dot) and AcSL16B (solid) in trifluoroethanol.

Ellipsometry. The ellipsometry was carried out by a MIZOJIRI Auto-Ellipsometers DHA-OLX/S at room temperature to determine the thickness of the pure peptide SAMs. The helium−neon laser at wavelength of 632.8 nm was used as incident light, and the incident angle of the light was set at 70°. The complex optical constant of peptide monolayers was assumed to be 1.50 + 0.00i. The thickness of the SAM was calculated automatically by using the equipped program (MEllipso). Measurements were carried out at more than 15 different spots of each peptide SAM. The reported results are the average of these measurements with an error within ±2 Å.

STM. STM measurements were performed by using a UNISOKU UPM-1100 under UHV ($\sim 10^{-9}$ Torr) at room temperature. All images were obtained in the constant current mode and recorded at high impedances (100 GΩ or higher) to maintain the tip position over the top surface of the monolayer and to prevent the monolayer surface from any mechanical damage, which allowed direct imaging of the molecular lattice. Mechanically polished PtIr tips were used as the scanning probe. The entire STM images shown here were unfiltered.

Results and Discussion

Conformation of Peptides in Solution. Conformation of the synthesized peptides in solution was examined by CD measurement. CD spectra of AcSL12B and AcSL16B are shown in Figure 2. These peptides show a double-minimum profile, which

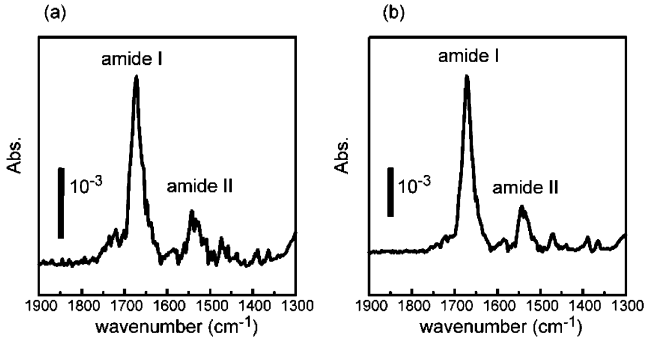

Figure 3. FTIR RAS spectra of the single-component helical peptide SAMs of (a) SL12B and (b) SL16B.

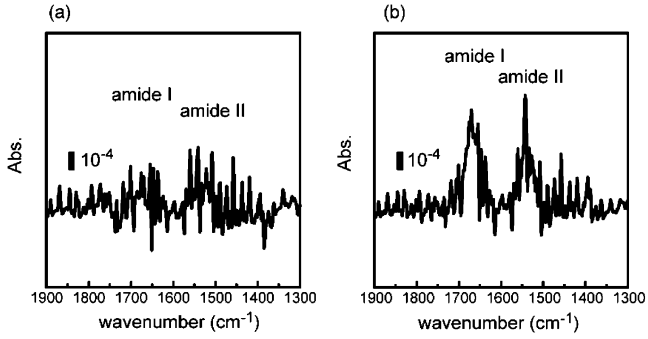

Figure 4. FTIR RAS spectra of the bicomponent SAMs composed of dodecanethiol and the helical peptide of (a) SL12B and (b) SL16B.

is characteristic of an α-helical structure.[16,17] The helix content of AcSL16B was larger than that of AcSL12B, showing that the longer peptide chain favors α-helical conformation which is in agreement with our previous results.[12c,14]

Characterization of the SAMs

(a) Single-Component Peptide Monolayer. Molecular orientation of the helical peptide SAMs was evaluated by FTIR RAS. Figure 3 represents the FTIR RAS spectra of the single component helical peptide SAMs. Amide I and amide II bands of the peptide SAMs appeared at 1670 and 1542 cm^{-1}, respectively, which is assigned to the amide bands of α-helical conformation.[18] α-Helical conformation of these peptides in the SAM is consistent with our previous reports, showing that Aib-containing peptides adopt a stable α-helical conformation on substrate with forming a well-packed molecular assembly.[14,19] Further, an intense absorption of amide I and a weak absorption of amide II suggest a vertical orientation of the helix to the surface. On the basis of the absorbance intensity ratio of amide I/amide II in the RAS spectra, the tilt angles of the helix axis from the surface normal were calculated by using eq 1 to be 34 and 32° for the SL12B and SL16B SAMs, respectively. On the other hand, film thicknesses of these SAMs were measured by ellipsometry to be 20.7 and 27.9 Å for SL12B and SL16B SAMs, respectively. These values fit in just the middle of the range of the thicknesses, 17−27 Å for SL12B and 23−32 Å for SL16B, which are calculated under constraints of the helical conformation and the tilt angles from FTIR RAS. The range of the thickness in the calculation is due to the conformational freedom at the terminal groups, the thiophenyl linker, and the benzyl ester group. These results indicate that both helical peptides stood nearly vertically in the peptide SAMs.

(b) Bicomponent Monolayer. The bicomponent SAMs were prepared by incubation of the dodecanethiolate SAM or the octanethiolate SAM with an ethanol solution of the helical peptides for 24 h at room temperature. FTIR RAS spectra of the bicomponent SAMs showed amide I and II bands around 1665 and 1540 cm^{-1}, respectively (Figures 4 and 5), indicating that the peptides can be incorporated into the alkanethiolate SAM with taking α-helical conformation. However, the absorption intensities were weak in the case of the peptide incorporation into the dodecanethiolate SAM despite of the long incubation time (Figure 4). Only the qualitative RAS analysis is allowed for the bicomponent SAM with the dodecanethiol. The low density of the peptide molecules in the dodecanethiolate SAMs suggests that the peptide molecules are incorporated mainly into the defects of the dodecanetiolate SAM and that the replacement of the dodecanetiol with the peptide should occur less frequently. The helical peptides easily associate together in ethanol solution to form peptide assemblies, which are hard to bind to the gold surface covered by the dodecanthiolate SAM.

On the other hand, the amide band intensities were adequate when the octanethiolate SAM was used as a host matrix monolayer (Figure 5). Loose molecular packing of the octanethiolate SAM could accept more helical peptide molecules than the dodecanethiolate SAM. To gain further information on the formation of the bicomponent SAMs such as preservation of helical conformation of peptide and ordering of matrix octanethiolate SAM, the bicomponent SAMs were prepared with changing the incubation time of the octanethiolate SAM with the peptide solution. Figure 5 shows FTIR RAS spectra of bicomponent SAMs with changing the incubation time from 1 to 24 h including the octanethiolate SAM and the peptide SAM.

In Figure 5a, the amide I and II bands of the peptide appeared around 1670 and 1542 cm^{-1}, and no shift of the peak position was observed with changing the incubation time. The incorporated peptide retained the helical conformation in the octanethiol SAM. IR signals from the incorporated peptide appeared quickly even after 1 h incubation, and reached a saturated level after 3 h incubation (Figure 5c). Amide A band of the peptide was observed around 3300 cm^{-1}, indicating that NH is involved in hydrogen bonding. The C−H stretching of the alkyl chain appeared around 2900 cm^{-1} (Figure 5b). Analysis of the methylene antisymmetric (d^-) and methylene symmetric (d^+) stretching bands of the alkyl chains provides information of the film structure of alkanethiol in the mixed SAMs.[7b,d] The octanethiol SAM gave a d^- signal at 2919 cm^{-1}.[20] In the bicomponent SAM, the d^- peak appeared at the same wavenumber, suggesting that the structure of the octanethiolate SAM was not disordered significantly by the incorporation of the peptide molecules into the SAM.

STM Observation of Single Helical Peptide. We previously reported a constant-current UHV STM image of the peptide SAM, which showed large terraces and monatomic steps due to the underlying Au(111) surface.[21] This image is a good evidence for formation of a flat and homogeneous peptide monolayer through Au−S linkage without significant defects. However, a single helical peptide molecule or a molecular array in the SAMs was not observable even at the high-resolution STM mode. Another group, which reported the SPM observation of the helical peptide SAM, has not succeeded in the observation of a single peptide molecule either.[22] In the case of the helical peptide SAM, it is difficult to observe a single molecule probably due to the occurrence of intermolecular lateral electron hopping, which makes the molecular imaging ambiguous.

Figure 6 shows the UHV STM images of the bicomponent SAMs of SL12B or SL16B and dodecanethiol. These images

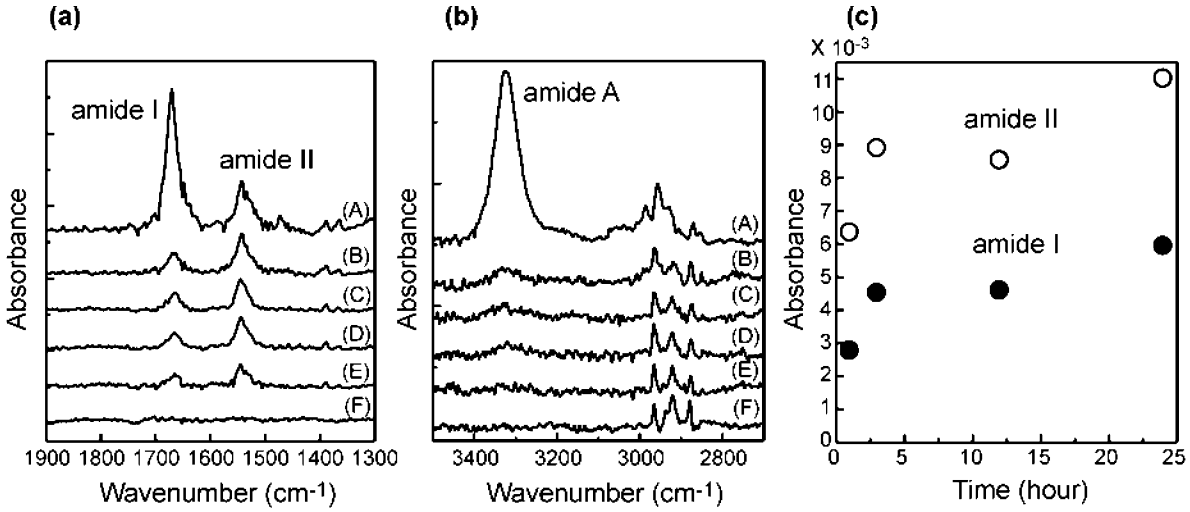

Figure 5. FTIR RAS spectra of the octanethiol monolayer and the bicomponent SAMs with changing incubation time with a SL16B solution: (A) the SL16B SAM, incubation in a SL16B solution for (B) 24 h, (C) 12 h, (D) 3 h, (E) 1 h, and (F) the octanethiol SAM. The Figures show (a) the amide I and II region, (b) the amide A region, and (c) the intensity changes of the amide I and II bands with incubation time.

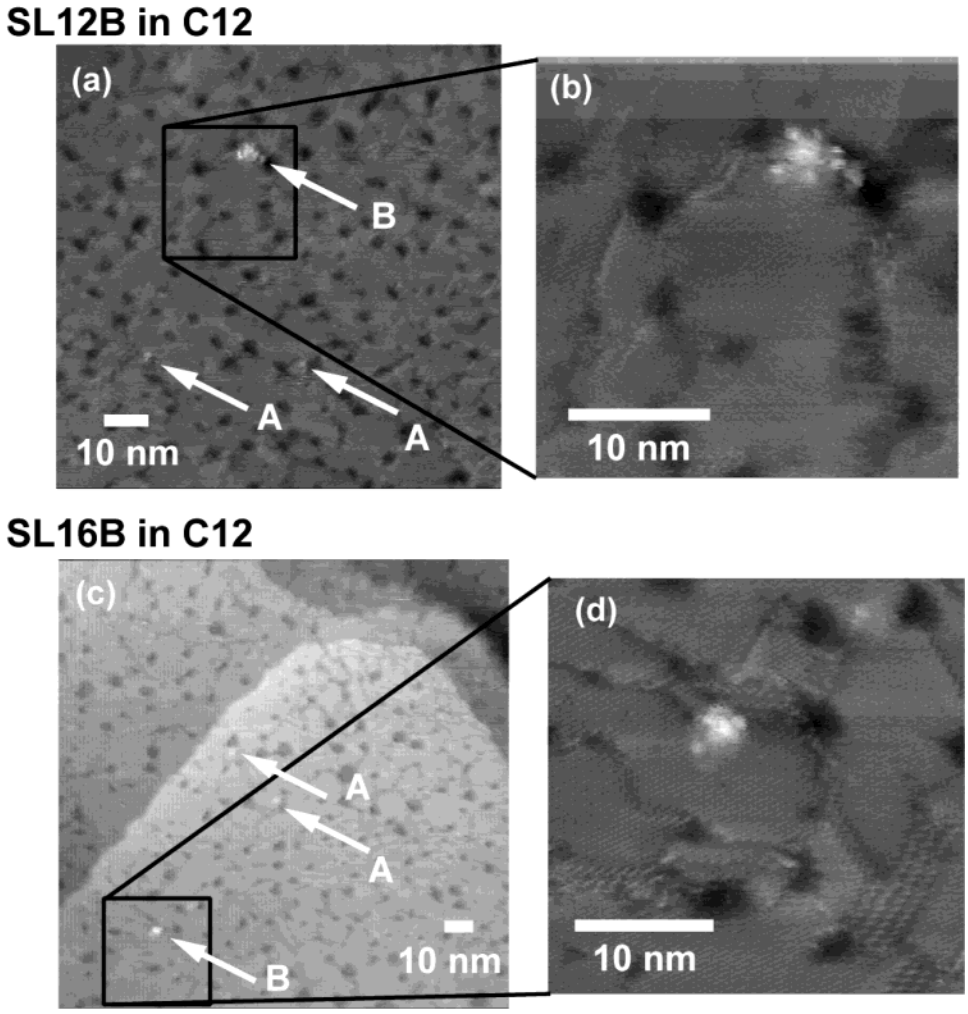

Figure 6. Constant current STM image of SL12B (a), (b) and SL16B (c), (d) incorporated in the dodecanethiol SAM. (a) and (c) Large area image of the bicomponent SAMs. Arrows A and B indicate the protrusions of the helical peptides of different sizes. (b) and (d) Magnified image of the area indicated by the square in (a) and (c). These images were recorded with sample bias of 1.0−1.6 V and tunneling set current of 3.0−5.4 pA.

show typical characteristics of the alkanethiol SAMs: the film domain boundaries, vacancy islands which are usually observed for monolayers prepared at room temperature, Au substrate terraces separated by single atom steps, and the $(\sqrt{3} \times \sqrt{3})$ R30° hexagonal structure.[23] Notably, the bright spots dispersed in the dodecanethiol SAM were clearly observed in the STM images. The sizes of these spots change apparently from place to place in the flat terraces (arrow A and B in parts a and c of Figure 6). The large spots (3∼4 nm in diameter) observed in these STM images are shown to be composed of a bundle of

small dots (approximately 1 nm in diameter) in the higher-resolution images (parts b and d of Figure 6). The diameter of each dot observed in the high-resolution images agrees well with the diameter of helix (ca. 1.3 nm), indicating that each dot represents a single helical peptide protruding from the surrounding dodecanethiol SAM. The helical peptides are incorporated probably into the monolayer domain boundaries with forming a bundle structure. Each dot looks very similar in the image, suggesting that the bundle structure is formed due to regular association of the helices in a parallel arrangement. Although STM images are a convolution of the tip shape and surface structures and it is always difficult to distinguish a single molecule from the matrix monolayer,[7] a single helical peptide molecule was successfully observed in our study with using the dodecanethiol SAM as a matrix of the peptide. We have also observed the helix bundles at some places in the bicomponent SAM with octanethiol. However, the octanetiolate matrix was not homogeneous; the alkyl chains were lying flat in the some regions and standing in the other. This arises from the fact that the length of octanethiolate is critical for the molecular orientation on gold. We therefore focus our attention on the bicomponent SAM with dodecanethiol.

Average height differences of the helical peptide from the surrounding dodecanethiol monolayer in the STM image were approximately 2.5 Å for the SL12B mixed SAM and 4.1 Å for the SL16B mixed SAM. On the other hand, the physical height differences between dodecanethiol and the peptide were calculated to be 2−12 Å for SL12B and 7−17 Å for SL16B on the basis of their molecular structures, assuming that the each helical peptide takes the same orientation as the dodecanethiol molecules (∼30° from the surface normal) in the SAMs and the conformational freedom is allowed at the terminal moieties. In the case of the bicomponent SAM with SL12B, the height difference by STM is agreeable with the calculated difference. However, the height difference in the bicomponent SAM with SL16B by STM is smaller than the calculated difference. The bicomponent SAM with SL12B was observed under the conditions typically of the applied voltage of 1 V and the tunneling current set of 5 pA (200 GΩ), while the SAM with SL16B was analyzed under more strict conditions, the applied voltage of 1.7 V and the current of 2.5 pA (∼700 GΩ). The vacuum gap between the STM tip and the surface of the dodecanethiol SAM was reported to be 1.3 Å under the conditions for the bicomponent SAM with SL12B.[7c] However, the vacuum gap under the strict conditions for the bicomponent SAM with SL16B should become much wider over the dodecanethiol. If the STM tip takes a position just above the SL16B molecule nearly without the vacuum gap, the height difference between SL16B and the dodecanethiol comes to be smaller than that of the real height difference. This should be the case of the STM measurement of the bicomponent SAM with SL16B. It is hard to say whether the STM tip is well controlled above the SAM of such a long molecule. Indeed, the tip sometimes scratched the SL16B molecules as shown in Figure 7. Probably, the helical peptide of 3−4 nm in length is critical for STM observation.

The number of the observed bright spots was relatively small, but it increased to some extent with changing the preparative condition. The difficulty of the incorporation of the helical peptides into the defects in the alkanethiol SAM may be due to a steric factor, because the helical peptides possess an assembling property into a bundle structure. To increase the number of the incorporated peptide molecules, chloroform was used as solvent for preparation of the bicomponent SAM of

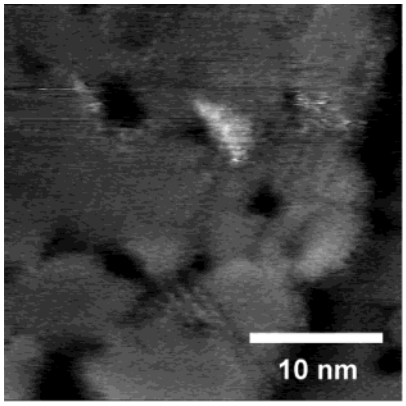

Figure 7. Constant current STM image of SL16B where the STM tip scratched the peptides during the scanning. The image is distorted in the *x* direction (scanning direction) when the tip scanned over SL16B molecules. This image was recorded with a sample bias of 1.7 V and tunneling current set of 2.5 pA.

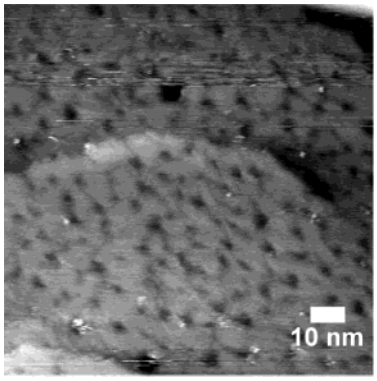

Figure 8. Constant current STM image of SL16B in the dodecanethiol SAM. Many bright spots were observed compared with Figure 6. This image was recorded with a sample bias of 1.6 V and tunneling current set of 4.0 pA.

SL16B and dodecanethiol. In chloroform, which is a good solvent for the peptide, the helical peptide should be molecularly dispersed. In fact, more bright spots were observed in Figure 8, indicating that solvent for preparation of the SAM affected the amount of the incorporated peptide molecules.

It is noteworthy that a cylindrically long molecule of 3∼4 nm length standing vertically on the surface was observed by STM. This observation implies that electron transfer occurs over a long distance through the helical peptide. Even though dominant contribution of the electron-transfer mechanism was not determined at this time, this result is consistent with the previous report that helical peptides have the ability to mediate a long-range electron transfer.[12d] SPM observation of a single molecule has been so far reported with various molecular wire candidates with help of the alkanethiol SAM as a matrix,[7,8] and the long molecules up to 4 nm were observed. These are π-conjugated oligo(phenylene-ethynylene) derivatives[7b,d] and dithiolated carotenoid,[8c] and electron transfer occurs by direct tunneling for these molecules.[24] Previously, the hopping mechanism was used for explanation of the long-range electron transfer across the helical peptide.[12d] However, in the present case, the helical peptide was set under a high bias voltage, over 1 V, which probably makes the coherent electron tunneling possible even for the long helical peptide because of the moderate attenuation factor, β. We are currently studying further on their electronic properties by scanning tunneling spectroscopy and CP-AFM.

Conclusion

We prepared the bicomponent SAMs by incorporation of the helical peptides into the dodecanethiol monolayer. FTIR RAS showed the incorporation of the peptide into the alkanethiol SAM did not disturb the conformation of the peptide and the film structure of alkanethiolate SAM. Further, we succeeded in observation of a single helical peptide molecule of 3∼4 nm length in the SAMs by STM, and confirmed the formation of the helix bundle. These results indicate that the electron transfer over a long distance is embodied in the helical peptides.

Acknowledgment. This work is partly supported by a Grant-in-Aid for Scientific Research B (12450372), Priority Areas Research B (Construction of Dynamic Redox Systems Based on Nano-Space Control), from the Ministry of Education, Culture, Sports, Science, and Technology, Japan.

References and Notes

(1) (a) Joachim, C.; Gimzewski, J. K.; Aviram, A. *Nature* **2000**, *408*, 541−548. (b) Carroll, R. L.; Gorman, C. B. *Angew. Chem., Int. Ed.* **2002**, *41*, 4378−4400. (c) Nitzan, A.; Ratner, M. A.; *Science* **2003**, *300*, 1384−1389. (d) Adams, D. M.; Brus, L.; Chidsey, C. E. D.; Creager, S.; Creutz, C.; Kagan, C. R.; Kamat, P. V.; Lieberman, M.; Lindsay, S.; Marcus, R. A.; Metzger, R. M.; Michel-Beyerle, M. E.; Miller, J. R.; Newton, M. D.; Rolison, D. R.; Sankey, O.; Schanze, K. S.; Yardley, J.; Zhu, X. *J. Phys. Chem. B* **2003**, *107*, 6668−6697.

(2) (a) Reed, M. A.; Zhou, C.; Muller, C. J.; Burgin, T. P.; Tour, J. M. *Science* **1997**, *278*, 252−254. (b) Smit, R. H. M.; Noat, Y.; Untiedt, C.; Lang, N. D.; van Hermert, M. C.; van Ruitenbeek, J. M. *Nature* **2002**, *419*, 906−909.

(3) (a) Park, J.; Pasupathy, A. N.; Goldsmith, J. I.; Chang, C.; Yaish, Y.; Petta, J. R.; Rinkoski, M.; Sthna, J. P.; Abruna, H. D.; McEuen, P. L.; Ralph, D. C. *Nature* **2002**, *417*, 722−725. (b) Liang, W.; Shores, M. P.; Bockrath, M.; Long, J. R.; Park, H. *Nature* **2002**, *417*, 725−729.

(4) (a) Slowinski, K.; Majda, M. *J. Electroanal. Chem.* **2000**, *491*, 139−147. (b) Rampi, M. A.; Whitesides, G. M. *Chem. Phys.* **2002**, *281*, 373−391.

(5) (a) Chen, J.; Reed, M. A.; Rawlett, A. M.; Tour, J. M. *Science* **1999**, *286*, 1550−1552. (b) Chen, J.; Wang, W.; Reed, M. A.; Rawleet, A. M.; Price, D. W.; Tour, J. M. *Appl. Phys. Lett.* **2000**, *77*, 1224−1226. (c) Chen, J.; Reed, M. A.; Rawleet, A. M.; Price, D. W.; Tour, J. M. *Appl. Phys. Lett.* **2001**, *78*, 3735−3737. (d) Wang, W.; Lee, T.; Reed. M. A.; *Phys. Rev. B* **2003**, *68*, 035416.

(6) (a) Kushmerick, J. G.; Holt, D. B.; Pollack, S. K.; Ratner, M. A.; Yang, J. C.; Schull, T. L.; Naciri, J.; Moore, M. H.; Shashidhar, R. *J. Am. Chem. Soc.* **2002**, *124*, 10654−10655. (b) Kushmerick, J. G.; Holt, D. B.; Yang, J. C.; Naciri, J.; Moore, M. H.; Shashidhar, R. *Phys. Rev. Lett.* **2002**, *89*, 086802.

(7) (a) Bumm, L. A.; Arnold, J. J.; Cygan, M. T.; Dunbar, T. D.; Burgin, T. P.; Jones, L., II; Allara, D. L.; Tour, J. M.; Weiss, P. S. *Science* **1996**, *271*, 1705−1707. (b) Cygan, M. T.; Dunbar, T. D.; Arnold, J. J.; Bumm, L. A.; Shedlock, N. F.; Burgin, T. P.; Jones, L., II; Allara, D. L.; Tour, J. M.; Weiss, P. S. *J. Am. Chem. Soc.* **1998**, *120*, 2721−2732. (c) Bumm, L. A.; Arnold, J. J.; Dunbar, T. D.; Allara, D. L.; Weiss, P. S. *J. Phys. Chem. B* **1999**, *103*, 8122−8127. (d) Dunbar, T. D.; Cygan, M. T.; Bumm, L. A.; McCarty, G. S.; Burgin, T. P.; Reinerth, W. A.; Jones, L., II; Jackiw, J. J.; Tour, J. M.; Weiss, P. S.; Allara, D. L. *J. Phys. Chem. B* **2000**, *104*, 4880−4893.

(8) (a) Cui, X. D.; Primak, A.; Zarate, X.; Tomfohr, J.; Sankey, O. F.; Moore, A. L.; Moore, T. A.; Gust, D.; Harris, G.; Lindsay, S. M. *Science* **2001**, *294*, 571−574. (b) Cui, X. D.; Zarate, X.; Tomfohr, J.; Sankey, O. F.; Primak, A.; Moore, A. L.; Moore, T. A.; Gust, D.; Harris, G.; Lindsay, S. M. *Nanotechnology* **2002**, *13*, 5−14. (c) Ramachandran, G. K.; Tomfohr, J. K.; Li, J.; Sankey, O.; Zarate, X.; Primak, A.; Terazono, Y.; Moore, T. A.; Moore, A. L.; Gust, D.; Nagahara, L. A.; Linsay, S. M. *J. Phys. Chem. B* **2003**, *107*, 6162−6169.

(9) (a) Giese, B.; Spichty, M. *ChemPhysChem* **2000**, *1*, 195−198. (b) Giese, B.; Amaudrut, J.; Kohler, A.-K.; Spormann, M.; Wessely, S. *Nature* **2001**, *412*, 318−320.

(10) Page, C. C.; Moser, C. C.; Chen, X. X.; Dutton, P. L. *Nature* **1999**, *402*, 47−52.

(11) (a) Winkler, J. R.; Di Bilio, A. J.; Farrow, N. A.; Richards, J. H.; Gray, H. B. *Pure Appl. Chem.* **1999**, *71*, 1753−1764. (b) Kornilova, A. Y.; Wishart, J. F.; Xiao, W.; Lasey, R. C.; Fedorova, A.; Shin, Y.-K.; Ogawa, M. Y. *J. Am. Chem. Soc.* **2000**, *122*, 7999−8006. (c) Sisido, M.; Hoshino, S.; Kusano, H.; Kuragaki, M.; Makino, M.; Sasaki, H.; Smith, T. A.; Ghiggino, K. P. *J. Phys. Chem. B* **2001**, *105*, 10407−10415. (d) Zheng, X.; Stuchebrukhov, A. A. *J. Phys. Chem. B* **2003**, *107*, 6621−6628. (e) Zheng, Y.; Case, M. A.; Wishart, J. F.; McLendon, G. L. *J. Phys. Chem. B* **2003**, *107*, 7288−7292. (f) Fedorova, A.; Chaudhari, A.; Ogawa, M. Y. *J. Am. Chem. Soc.* **2003**, *125*, 357−362. (g) Shin, Y.-G. K.; Newton, M. D.; Isied, S. S. *J. Am. Chem. Soc.* **2003**, *125*, 3722−3732.

(12) (a) Hol, W. G. *J. Prog. Biophys. Mol. Biol.* **1985**, *45*, 149−195. (b) Galoppini, E.; Fox, M. A. *J. Am. Chem. Soc.* **1996**, *118*, 2299−2300. (c) Morita, T.; Kimura, S.; Kobayashi, S.; Imanishi, Y. *J. Am. Chem. Soc.* **2000**, *122*, 2850−2859. (d) Morita, T.; Kimura, S. *J. Am. Chem. Soc.* **2003**, *125*, 8732−8733.

(13) Helical peptide conformation is kept under a high-vacuum system. See: Miura, Y.; Kimura, S.; Kobayashi, S.; Iwamoto, M.; Imanishi, Y.; Umemura, J. *Chem. Phys. Lett.* **1999**, *315*, 1−6.

(14) Miura, Y.; Kimura, S.; Imanishi, Y.; Umemura, J. *Langmuir* **1998**, *14*, 6935−6940.

(15) Tsuboi, M. *J. Polym. Sci.* **1962**, *59*, 139−153.

(16) Holzwarth, G.; Doty, P. *J. Am. Chem. Soc.* **1965**, *87*, 218−228.

(17) Chen, Y. H.; Yang, J. T.; Martinez, H. M. *Biochemistry* **1972**, *11*, 4120−4131.

(18) Kennedy, D. F.; Chrisma, M.; Chapman, T. D. *Biochemistry* **1991**, *30*, 6541−6548.

(19) (a) Fujita, K.; Kimura, S.; Imanishi, Y.; Rump, E.; Ringsdorf, H. *Langmuir* **1994**, *10*, 2731−2735. (b) Fujita, K.; Kimura, S.; Imanishi, Y.; Rump, E.; Ringsdorf, H. *Langmuir* **1995**, *11*, 253−258. (c) Fujita, K.; Kimura, S.; Imanishi, Y.; Okamura, E.; Umemura, J. *Langmuir* **1995**, *11*, 1675−1679.

(20) Porter, M. D.; Bright, T. B.; Allara, D. L.; Chidsey, C. D. E. *J. Am. Chem. Soc.* **1987**, *109*, 3559−3568.

(21) Kitagawa, K.; Morita, T.; Kawasaki, M.; Kimura, S. *J. Polym. Sci. A* **2003**, *41*, 3493−3500.

(22) (a) Fujita, K.; Bunjes, N.; Nakajima, K.; Hara, M.; Sasabe, H.; Knoll, W. *Langmuir* **1998**, *14*, 6167−6172. (b) Brask, J.; Wackerbarth, H.; Jensen, K. J.; Zhang, J.; Chorkendorff, L.; Ulstrup, J. *J. Am. Chem. Soc.* **2003**, *125*, 94−104. (c) Case, M. A.; McLendon, G. L.; Hu, Y.; Vanderlick, T. K.; Scoles, G. *Nano. Lett.* **2003**, *3*, 425−429.

(23) Poirier, G. E. *Chem. Rev.* **1997**, *97*, 1117−1127.

(24) Recent study showed electron transported via localized molecular orbitals for phenylene-ethynylene oligomer. See: Fan, F.-R. F.; Lai, R. Y.; Cornil, J.; Karzazi, Y.; Brédas, J.-L.; Cai, L.; Cheng, L.; Yao, Y.; Price, D. W., Jr.; Dirk, S. M.; Tour, J. M.; Bard, A. J. *J. Am. Chem. Soc.* **2004**, *126*, 2568−2573.